A stochastic model of torque in von Karman swirling flow

Nicolas Leprovost, Louis Marié, Bérengère Dubrulle

EPJ manuscript No.
(will be inserted by the editor)

A stochastic model of torques in von Karman swirling flow

N. Leprovost, L. Marié, and B. Dubrulle

Groupe Instabilité et Turbulence,

CEA/DSM/DRECAM/SPEC and CNRS. URA 2464 F-91191 Gif sur Yvette Cedex, France

e-mail: bdubru@drecam.saclay.cea.fr

Received: date / Revised version: date

Abstract. A stochastic model is derived to predict the turbulent torque produced by a swirling flow. It is a simple Langevin process, with a colored noise. Using the unified colored noise approximation, we derive analytically the PDF of the fluctuations of injected power in two forcing regimes: constant angular velocity or constant applied torque. In the limit of small velocity fluctuations and vanishing inertia, we predict that the injected power fluctuates twice less in the case of constant torque than in the case of constant angular velocity forcing. The model is further tested against experimental data in a von Karman device filled with water. It is shown to allow for a parameter-free prediction of the PDF of power fluctuations in the case where the forcing is made at constant torque. A physical interpretation of our model is finally given, using a quasi-linear model of turbulence.

PACS. 47.27 Turbulent flows, convection and heat transfer – 47.27 Eq Turbulence modeling

1 Introduction

1.1 Historical background

A classical topic in turbulence research is the computation of global transport properties connected with the macroscopic result of turbulent motions at microscopic scales. These motions are characterized by very rapid characteristic time scales, and can be considered, from a macroscopic point of view, as fluctuations. The "conventional approach" consists in modelling the mean value of non linear functions of these fluctuations in terms of averaged quantities, the most famous example being the turbulent viscosity [1]. However, this will only give evolution equations for averaged quantities and nothing can be predict on the shape of the fluctuations (for example their probability distribution function). An alternative approach is to consider these fluctuations as noises and most of problems

dealing with turbulent transport could then be solved if one were able to prescribe the statistics of this noise, as a function of some global properties of the flow. A priori, this can be done in two ways. Firstly, by assuming the probability density function of the noise to be known. This approach has been pioneered by [2], starting from Navier-Stokes equations, but its solution has encountered considerable technical difficulties [3]. In some instances (e.g. for velocity increments) where the noise obeys a Markov property, it is however possible to derive an approximate Fokker-Planck equation by fitting of the turbulent data [4,5,6,7]. Another way to prescribe the statistics of the noise is through a stochastic equation, taking for example the Langevin equation. In some sense, this approach has been pioneered by [8], who assumes a Gaussian white noise statistics for the acceleration. Refinements of this model have later been proposed by [9,10,11,12] to account for intermittency of small scale velocity increments.

1.2 The Langevin approach

From a practical (numerical) point of view, Langevin approaches are often easier to implement, since they only involve integration of ordinary differential equation, in contrast with Fokker-Planck methods which involve partial differential equation in a high dimension space (the phase space). From the theoretical point of view, the link between the two approaches is not straightforward: it can be shown that different Langevin models can in fact lead to the same Fokker-Planck equation, so that the correspondence between the noise property and the fluid equations of motions is not always obvious. In that respect, it would be interesting to develop some sort of systematic procedure to derive a Langevin equation for the noise starting from the Navier-Stokes equations. Recently, [13, 14,15] provided evidence that the small scales of a turbulent flow are mostly slaved to the large scale, and follow a quasi-linear dynamic [16,17,18,19]. This dynamics is described by the rapid Distortion Theory, see e.g. [20,21,22, 23,24]. This led us to propose a new turbulent model for small scale turbulence, in which the velocity is given as a solution of a linear stochastic equation of Langevin type [25]. A preliminary validation of the model was done by comparison with direct numerical simulation of isotropic 3D turbulence. This kind of turbulence is however seldom realized in real life applications. Therefore, a validation of this type of model in non-isotropic, non-homogeneous situations would be most welcome.

1.3 A model experiment

A good prototype of this type of flow is the so-called von Karman flow, the flow between two coaxial rotating disks (cf figure 1). This simple device allows both for turbulence with a very large Reynolds number and easy access to global transport properties via torque measurements focusing either on averaged quantities [26,27,28] or probability distributions [29]. The statistical analysis revealed a rich and complex connection between the energy injection and dissipation, reflecting the non-trivial coupling between the macroscopic scale and the underlying microscopic turbulent noise. For example, Titon and Cadot [29]

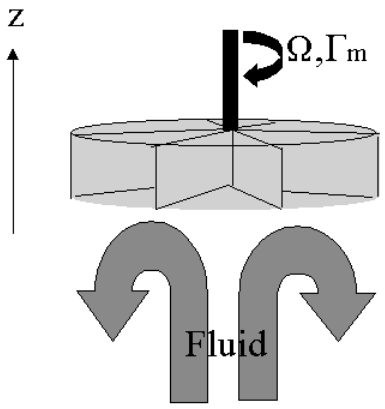

Fig. 1. Von Karman experimental setup, Ω and Γ_m are respectively the angular velocity of the disk and the torque supplied by the engines.

studied power injection statistics, in the regime obtained when the disks are counter-rotating at same angular velocity. In this case, the stationary state is made of two cells with opposite azimuthal velocity. The measurements of Titon and Cadot cover a range of Reynolds number between 2×10^4 to 5×10^5, in two regimes: in the first one, the angular velocity of the stirrers is constant (Ω-mode); in the second one, the mechanical torque is kept constant in time (Γ-mode). For each mode, the shape of the injected power statistics is found independent of the Reynolds number. It is approximately Gaussian, with a slight asymmetry. While the rate of fluctuations of the injected power is independent of the Reynolds number within each mode, it is found to depend strongly on the type of mode: it is twice larger in the first regime than in the second one.

In stationary regime, one expects the energy injection to be equal on average to the energy dissipations. Yet, the two processes clearly differ: the nearly Gaussian character of the PDF's of energy injection fluctuations contrasts with the very non-Gaussian (log-normal) behavior observed for energy dissipation. Also, the strong dependence of the statistics on the forcing mechanism goes against the universality assumption usually applied on energy dissipation in classical theories of turbulence. These interesting differences are far from being completely understood, from a theoretical point of view. In a recent work, Aumaitre et al [30] showed that the statistics of the injected power obey a "fluctuation theorem", enabling to connect the probabilities of positive and negative production rate during a given time interval (this characterizes the asymmetry of the curve). However, a rigorous proof of the theorem only applies to time-reversible systems, at variance with ordinary turbulence. Aumaitre et al [30] therefore also mention that their result could be just a consequence of the theory of large deviations [31,32].

1.4 Aim of the paper

These two examples illustrate clearly the complexity of the global transport properties occurring in the von Karman device. The questions we address in the present paper are: i) can we capture the main features of the transport through a simple Langevin model ? ii) can we make a link between this Langevin model and the Navier-Stokes equations through the quasi-linear model of turbulence of [16, 17,18,19,25] ?

We answer to these questions in two separate Sections, one devoted to the finding and analyzing of the Langevin model, and one devoted to its possible justifica-

tion through the turbulent model. To further test the basic hypothesis of the model, and to validate it thoroughly, we used confrontation with experimental data collected specifically for this purpose in the von Karman experimental device of Saclay, described in [33].

2 Ω-mode and the Langevin model

2.1 Momentum equation

To derive the simplest Langevin model compatible with the data, we may follow Titon and Cadot [29], and write the momentum balance equation for one stirrer (including blades and water trapped in it), as :

$$I\frac{d\Omega}{dt} = \Gamma_m(t) - \Gamma_f(t) \quad (1)$$

where I is the inertia of the disks (including the blades and the water trapped in it), Ω is the rotation velocity of the disk, Γ_m is the angular momentum supplied by the motors (the propeller) and Γ_f is the torque due to the fluid acting onto the propeller.

2.2 Derivation of the Langevin model

From a theoretical point of view, $\Gamma_f(t)$ is the turbulent contribution to be modeled as a noise. Its main properties can be easily specified by working in the Ω-mode, where $\Gamma_m = -\Gamma_f$, and study the signal delivered by the motor. From experiments performed with a von-Karman device working in water, regulated in Ω-mode ($\Omega = 59.6\ rad.s^{-1}$), one observe a roughly Gaussian distribution with a mean value proportional to Ω^2, with prefactor having the sign of Ω. We thus write $\Gamma_f = c\Omega|\Omega| - \xi$ where ξ is a Gaussian noise with zero mean, specified by its second order moment (the variance). To completely determine it, we extracted a temporal correlation for the mechanical torque (figure 2 shows this correlation versus time). One sees an oscillation at a frequency around 8.9 Hz (56.2 $rad.s^{-1}$), superposed to a rapid damping. On the other hand, the Fourier transform of the signal displays a rather wide ranging from 0 to about 9 Hz (Figure 3), instead of a well defined narrow peak, which would be characteristic of a meaningfull

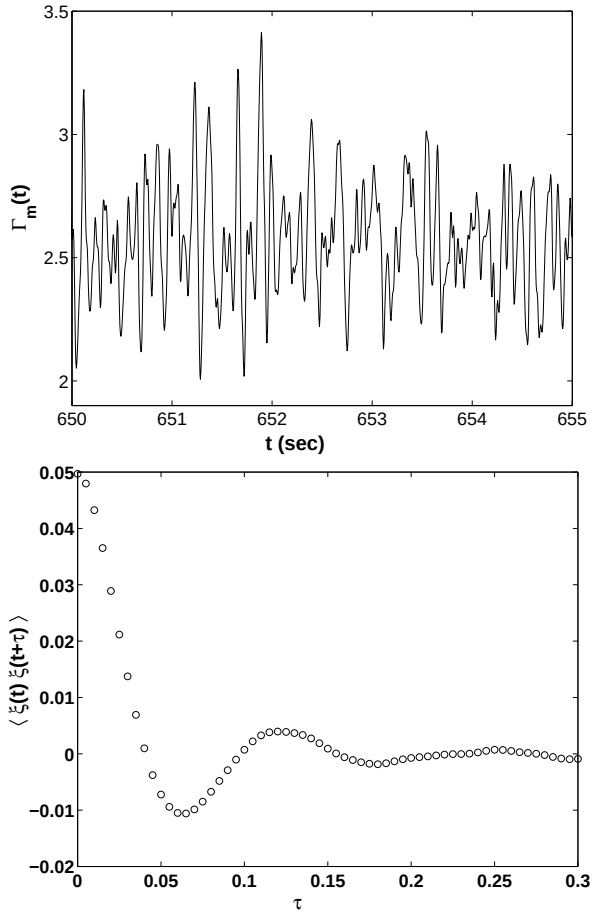

Fig. 2. Sketch of 5 seconds of torque signal from the Saclay experiment (top) and temporal correlation (bottom).

oscillation. Finally, we note that such oscillation is not visible in similar measurements performed in air [26]. It is therefore difficult to decide whether this oscillation is a real physical feature, or provoked by some experimental artefact.

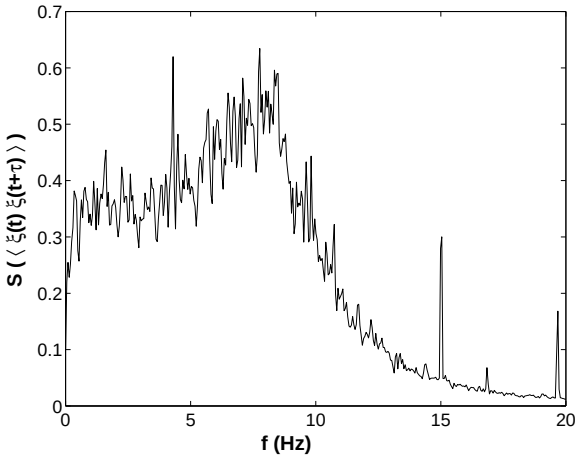

Fig. 3. Spectrum of the correlation function.

If the oscillating behavior of the correlation function is considered, the simplest Langevin model is the OWN (oscillating white noise) model:

$$\frac{d^2\xi}{dt^2} = -2\gamma\frac{d\xi}{dt} - \omega_0^2\xi + \Gamma(t)\ , \tag{2}$$

where $\langle\Gamma(t)\Gamma(t')\rangle = 2D_0\delta(t-t')$. This equation leads to a stationary gaussian distribution for ξ (thermal equilibrium) with variance $\langle\xi^2\rangle = D_0/(2\gamma\omega_0^2)$ and a temporal correlation $C(\tau) = \langle\xi(t+\tau)\xi(t)\rangle$ which reads:

$$C(\tau) = e^{-\gamma\tau}[A\cos(\sqrt{\omega_0^2-\gamma^2}\tau) + B\sin(\sqrt{\omega_0^2-\gamma^2}\tau)] \tag{3}$$

where $A = \langle\xi^2\rangle$ and $B = \gamma A/\sqrt{\omega_0^2-\gamma^2}$.

If, on the other hand, the oscillation is a spurious experimental artefact, the only physical property to take into account is the damping, which appears approximately exponential. The resulting Langevin equation is the EWN (exponential white noise) model:

$$\frac{d\xi}{dt} = -\frac{1}{\tau}\xi + \frac{\eta(t)}{\tau}\ , \qquad \langle\eta(t)\eta(t')\rangle = 2D\delta(t-t') \tag{4}$$

This leads to an exponentially decaying correlation function

$$C(\tau) = \frac{D}{\tau}\, e^{-\frac{t}{\tau}} \tag{5}$$

2.3 Calibration

The constants appearing in the models OWN and EWN can be found by fit on the PDF of torque measurements and correlation function. For the model OWN, we find;

$$\begin{aligned} \omega_0 &= 55.9\ rad.s^{-1}, \\ \gamma &= 24.1\ s^{-1} \\ D_0 &= 2\gamma\omega_0^2\langle\xi^2\rangle = 7.49\,10^3\ kg^2.m^4.s^{-7}, \\ c &= 7.42\,10^{-4}\ kg.m^2 \end{aligned} \tag{6}$$

while for the model EWN, we find:

$$\begin{aligned} \tau &= \frac{1}{\gamma} = 0.042\ s \\ D &= \tau\langle\xi^2\rangle = 2.1\,10^{-3}\ kg^2.m^4.s^{-3} \\ c &= 7.42\,10^{-4}\ kg.m^2 \end{aligned} \tag{7}$$

Our calibration can be checked by comparison between the model and the data is provided in Fig. 4: top for the PDF and bottom for the correlation function. One sees that the PDF are well reproduced with our choice of parameter. For the correlation functions, one sees that the model OWN captures well the first oscillation, but decreases a little bit too slowly.

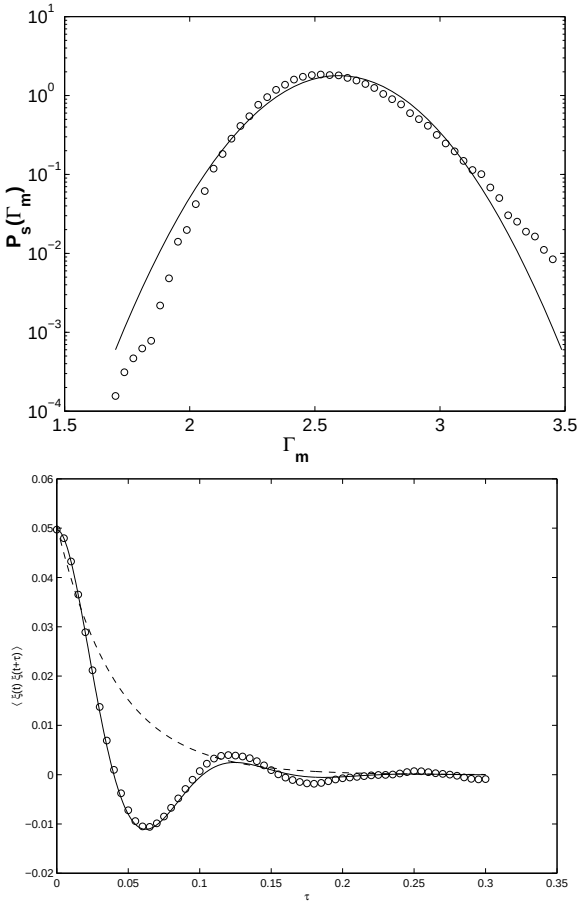

Fig. 4. PDF of the torque (top) and temporal correlation (bottom). The points are from the experiment, the solid line corresponds to the model OWN and the dashed line to the EWN model (concerning the PDF, both model give the same Gaussian distribution).

3 Predictions in Γ-mode

3.1 Numerical study of the model

The calibration of the model enables the determination of the probability distribution for angular velocity in the Γ-mode. In this case, $\Gamma_m = cte$ and the angular velocity becomes a stochastic variable, solution of the equation:

$$I\frac{d\Omega}{dt} = \Gamma_m - c|\Omega|\Omega + \xi(t) \tag{8}$$

where $\xi(t)$ is given by equation (2) or (5). Solutions of this coupled system of equation can be found using classical stochastic numerical methods [34]. The only trick arises for the OWN model whose dynamics is second order in time. In this case, we used the following numerical scheme:

$$\begin{aligned}\xi(t+\Delta t) &= \xi(t) + y(t)\Delta t \\ y(t+\Delta t) &= y(t) - \omega_0^2\xi(t)\Delta t - 2\gamma y(t)\Delta t + \Gamma(t) \\ \Omega(t+\Delta t) &= \Omega(t) + (\Gamma_m - c|\Omega(t)|\Omega(t))\frac{\Delta t}{I} + \xi(t)\frac{\Delta t}{I}\end{aligned} \tag{9}$$

In Fig. 5, we show an example of the resulting probability distribution function computed numerically using the two models, and with the constants calibrated on the data. In both cases, one obtain a PDF with a mean value $<\Omega>= 61.4\ rad.s^{-1}$, and some deviations from a Gaussian character. However, one sees that the two models are characterized by quite different variances. In a sense, this is quite surprising because the two models can be shown to exhibit interesting similarities under a simple approximation.

3.2 Overdamped approximation

Indeed, in the overdamped regime, one can neglect inertia in (2) so that the noise in the OWN model obeys:

$$\begin{aligned}\frac{d\xi}{dt} &= -\frac{1}{\tau}\xi + \frac{\eta(t)}{\tau}\,, \\ \tau &= \frac{2\gamma}{\omega_0^2}\,, \\ \langle\eta(t)\eta(t')\rangle &= \frac{2D_0}{\omega_0^4}\delta(t-t') = 2D\delta(t-t')\end{aligned} \tag{10}$$

One therefore recovers the equation for the EWN with slightly different parameters:

$$\tau = \frac{2\gamma}{\omega_0^2} = 0.015\ s\,, \tag{11}$$

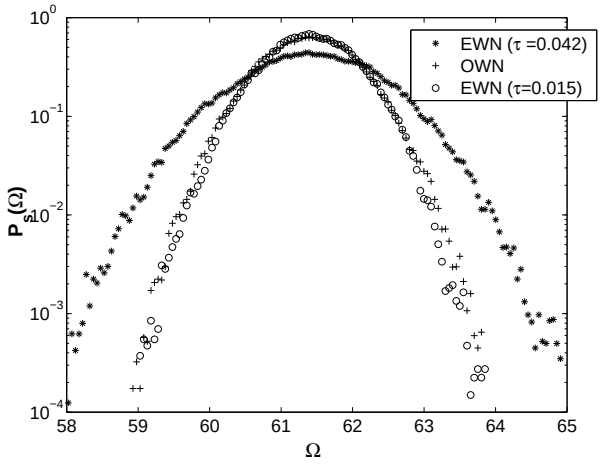

Fig. 5. PDF of the angular velocity computed in Γ-mode ($\Gamma_m = 2.8\ kg.m^2.s^{-2}$) numerically for the two models. The parameters values are that determined in the calibration and $I = 0.022\ kg.m^2$. We also show the numerical integration of the EWN model with values for τ et D corresponding to the overdamped approximation.

$$D = \frac{D_0}{\omega_0^4} = 7.67\,10^{-4}\ kg^2.m^4.s^{-3}$$
$$c = 7.42\,10^{-4}\ kg.m^2$$

The comparison between the PDF in the overdamped approximation (cf next section) and the PDF from the numerical simulation shows a good agreement. The present result therefore suggests that the large difference between the two models only comes from the different physical parameters. To understand the origin of the difference, we undertake an analytical investigation, using the EWN model.

3.3 Analytical study

3.3.1 Power in Ω-mode

In this regime, the power delivered by the propellers and the power injected in the flow are equal. In the sequel, we shall call this power $P_\Omega = P_1 = P_2 = c\Omega^3 + \xi\Omega$. We can immediately derive the PDF of P_Ω from ξ. It is a gaussian random variable with mean $c\Omega^3$and variance:

$$\delta P_\Omega^2 = \Omega^2\langle\xi^2\rangle = \frac{D\Omega^2}{\tau} \tag{12}$$

3.3.2 Power in Gammamode

To find the power in the gamma-mode, one must solve analytically the equation (8) with (5). A technical difficulty arises because ξ is not a δ-correlated process . However, under the unified colored noise approximation [35,36], one can compute the stationary PDF of Ω and get the following (cf appendix A):

$$P_s(\Omega) = N(I + 2c\tau|\Omega|) \times \tag{13}$$
$$\exp\frac{1}{D}[I\Omega(\Gamma_m - c\Omega^2\theta(\Omega)/3) + c\tau\Omega^2(\Gamma_m\theta(\Omega) - c\Omega^2/2)]$$

where θ is the sign function. The moment of this distribution cannot be computed analytically in general. The simplest approximation which allows analytical calculations is when the intensity of the noise is small, a regime that will be considered in the next section.

The small noise limit In this section we rewrite the probability density function for Ω in a dimensionless form: with $\chi = \sqrt{\frac{c}{\Gamma_m}}\Omega$, $R^2 = \frac{2D}{\tau\Gamma_m^2}$ and $S = \frac{2I}{\sqrt{c\Gamma_m}\tau}$, one has for the

stationary probability density of χ:

$$P_s(\chi) = N(|\chi| + \frac{S}{4}) \exp(-\frac{1}{R^2}[(\chi^2 - \theta(\chi))^2 - S\chi + \frac{S}{3}\theta(\chi)\chi^3]) \quad (14)$$

where N stands for the normalization.

In the appendix B, we used Laplace's method with $R \ll 1$ to compute the n-th order moment of the distribution (14):

$$< \chi^n >= 1 - \frac{R^2}{4(4+S)} n(2-n) + O(R^4) \quad (15)$$

From this expression, we are able to compute the standard deviation of the processus and recover a relation enlightened by [29]. In the limit of inertia (or equivalently S) going to zero, we have:

$$\begin{aligned} \delta P_\Gamma^2 &\equiv \Gamma_m^2[< \Omega^2 > - < \Omega >^2] \quad (16) \\ &= \Gamma_m^2 < \Omega >^2 [\frac{< \chi^2 >}{< \chi >^2} - 1] \\ &= \Gamma_m^2 \frac{R^2}{8} < \Omega >^2 = \frac{D}{4\tau} < \Omega >^2 = \frac{1}{4}\delta P_\Omega^2 \end{aligned}$$

This relation shows that in the limit where the inertia of the disk is going to zero, the fluctuations of power delivered by the motor are twice smaller in one of the mode of forcing, namely the Γ-mode as compared to the Ω-mode (with the same mean angular rotation rate). However, this relation has been derived under the assumption of vanishing noise. We now have to check if this relation holds when the noise becomes stronger and stronger. On figure 6, we plotted the quantity $\alpha = \frac{\delta P_\Gamma^2}{\delta P_\Omega^2} = \frac{2<\chi^2>-<\chi>^2}{R^2<\chi>^2}$ numerically computed from the expression (14) versus the adimensionalized inertia, S and simultaneously, the expression derived in appendix B, in the limit $R \ll 1$, $\alpha = \frac{1}{4+S}$. We see roughly that for $R < 1$, the preceding relation is in good agreement with the numerical calculations, whereas for $R > 1$, the two quantities diverge one from another. Furthermore, in this last situation, α is not close to $\frac{1}{4}$ as S is going to zero. The relation (16) is consequently only valid under the double assumption: $R \ll 1$ and $I \to 0$.

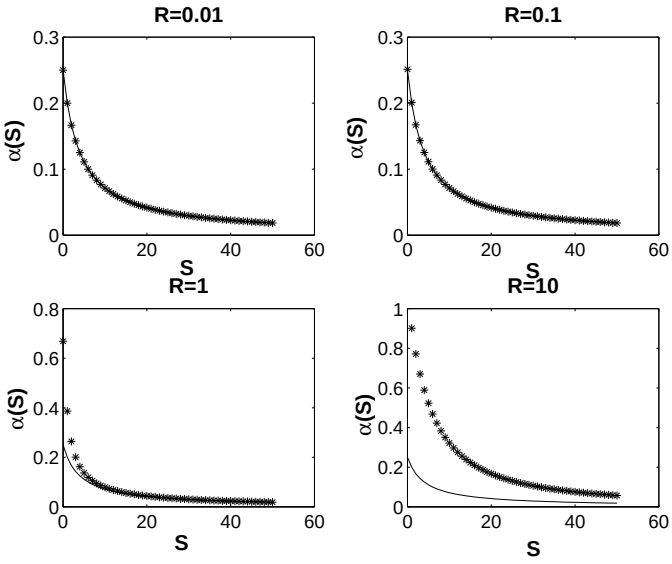

Fig. 6. Evolution of the parameter $\alpha = \frac{\delta P_\Gamma^2}{\delta P_\Omega^2}$ with S (i.e. the inertia) for different values of R (intensity of the noise. The points correspond to the numerical computation and the solid line to the approximate expression derived assuming the intensity of the noise was small.

In summary, we found in this section a relation linking the fluctuations of the injected power in two forcing regimes: one with constant velocity and one with constant torque. This relation is valid for vanishing inertia and states (eq. (16)) that the power fluctuation at constant velocity are twice larger as power fluctuations at constant torque. This relation has been empirically dis-

covered by Titon and Cadot [29] using experimental data, without discussion of its range of validity. With our model, we predict that this range is restricted to weak noise and weak inertia, as can be seen in figure 6.

Application Our analytical computation can be used to explain the difference between the two models. For this, we can compute the values of the parameter R and S for the two models, using the calibrated constants. In the model OWN, we find $R = 0.11$ and $S = 62.6$. This indeed corresponds to the weak noise limit, and from (36) we find $\delta\Omega^2 = [\langle\chi^2\rangle - \langle\chi\rangle^2]\Gamma_m/c = 0.34$. In the model EWN, we find $R = 0.11$ and $S = 23.3$. We therefore recover the same value for the noise intensity, but a quite different value for the adimensionalized inertia S. Using formula (36), this results in $\delta\Omega^2 = 0.84$, about twice bigger as the value for the OWN model ! This therefore explains the difference between the two models. It is therefore now interesting to compare this PDF with experimental data, to see which model is closer to the real distribution.

Comparison with experimental data On figure 7, we show the experimental data of the VKE experiment forced with a constant torque ($\Gamma_m = 2.8\ Kg.m^2.s^{-2}$) and in such a way that the mean angular velocity is roughly 60 $rad.s^{-1}$ (the exact value is 61.6 $rad.s^{-1}$). This is compared with the theoretical prediction for both the OWN and the EWN model. As one can see, the experimental curve agrees very well with the EWN model, but not with the OWN model. A OWN model can reproduce the data only provided a change of the parameters of the fit, e.g. a oscillation's frequency smaller by a factor of $\sqrt{3}$, or no oscillation at all. Indeed the spectrum of the correlation function of ξ in the Γ-regime shows no preferred frequency (figure 8).

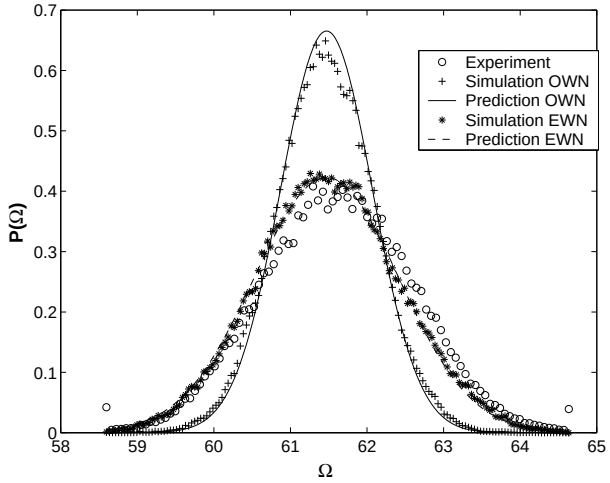

Fig. 7. Probability distribution for the angular velocity when the device is forced at constant torque ($\Gamma_m = 2.8\ kg.m^2.s^{-2}$) for the experiment, a simulation of equations (8) and (5), and for the theoretical predictions (13) in the overdamped case.

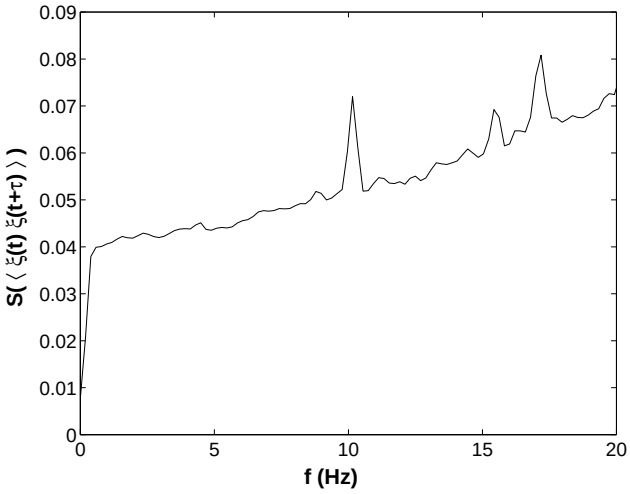

Fig. 8. Spectrum of the correlation function of ξ calculated in the Γ-mode.

In previous experiments of Von-Karman swirling flow, it has been observed that the skewness in Ω and Γ mode is of different sign. It is not possible to reproduce such a feature in our model since, by assumption, the skewness is zero in the Ω mode (gaussian noise). However, it is possible to investigate the skewness in Γ mode. To proceed, one needs to carry the Laplace method ut to terms in R^4 (one can check that the skewness vanishes up to order 2) and after straightforward calculations, it appears that the skewness is:

$$\frac{< (x- < x >)^3 >}{(< x^2 > - < x >^2)^{3/2}} = -\frac{R(12+S)}{\sqrt{2(4+S)^3}} \qquad (17)$$

This quantity is always negative, a result consistent with previous experimental observations (see for example [37]). In our experimental result, the skewness is measured to be -0.026. With the value of the parameters, our analytical prediction gives a value for the skewness of -0.019 for the EWN model, and -0.011 for the OWN model. Again, there is much better agreement between the experimental results and the EWN model, than with the OWN model in this regime. There are two possible explanation:

1. the oscillation detected is a pure experimental artefact, so that OWN has no physical origin
2. the frequency of oscillation is not an universal parameter and varies accordingly to the forcing regime.

Datas seem to select the second explanation. It is nevertheless interesting to understand better the physical difference between the two models, trying to pin-point its origin from the Navier-Stokes equations.

4 What can be said from a quasi-linear model of turbulence?

4.1 Basic equations

In the previous sections, we have derived a Langevin model for the turbulent torque Γ_f. In fact, this torque can be simply related to a component of the Reynolds stress through the angular momentum conservation, see e.g. Marié and Daviaud [33]:

$$\Gamma_f = \int_{\Sigma_p} \rho u_z u_\phi r dS \qquad (18)$$

Here Σ_p is the cross-section of the cylinder which closes the portion that is swept by the blades of the stirrer, and u_ϕ and u_z denote the azimuthal and vertical fluid velocity component. If we now separate the velocity into its mean $< u >$ and fluctuating u' contribution, we get:

$$\Gamma_f = \int_{\Sigma_p} \rho(< u_z >< u_\phi > + < u_z > u'_\phi + u'_z < u_\phi > + u'_z u'_\phi) r dS. \qquad (19)$$

The average of this expression gives the mean torque as:

$$< \Gamma_f >= \int_{\Sigma_p} \rho(< u_z >< u_\phi > + < u'_z u'_\phi >) r dS. \qquad (20)$$

This is a classical expression for the torque transport. It is easy to express it on pure dimensional ground as $< \Gamma_f >= -c|\Omega|\Omega$, where c is a drag coefficient. Our main interest is the fluctuating part of Γ_f, which will provide the noise contribution. It is:

$$\Gamma'_f = \int_{\Sigma_p} \rho(< u_z > u'_\phi + u'_z < u_\phi > + u'_z u'_\phi - < u'_z u'_\phi >) r dS. \qquad (21)$$

At this point, it is natural to assume that the difference $u'_z u'_\phi - < u'_z u'_\phi >$ (the fluctuating part of the Reynolds

stress) is small compared to the other two terms, which are both proportional to the average of a mean quantity. Also, since the fluctuating part varies over time scale much smaller than the mean part, it is easy to see that we must have:

$$D_t \Gamma'_f \approx \int_{\Sigma_p} \rho(< u_z > D_t u'_\phi + D_t u'_z < u_\phi >) r dS. \quad (22)$$

A model for the fluctuating torque variation will then be found provided one finds a model for the fluctuating velocity variations.

4.2 The quasi-linear approximation

To obtain the dynamical behavior of fluctuating velocities, we use the turbulent model of Laval, Dubrulle and Mc Williams [25] in which the velocity is given as a solution of a linear stochastic equation of Langevin type, valid for localized wave-packets, which may be summarized as:

$$D_t \hat{u}'_i = -\nu^t \mathbf{k}^2 \hat{u}'_i + B_{ij} \hat{u}'_j + \eta_i, \quad (23)$$

where B_{ij} is a linear operator depending only on the average velocity, ν_t is a turbulent viscosity, and

$$\hat{u}'(\mathbf{x}, \mathbf{k}, t) = \int g(|\mathbf{x} - \mathbf{x}'|) e^{i\mathbf{k}\cdot(\mathbf{x}-\mathbf{x}')} \mathbf{u}'(\mathbf{x}', t) d\mathbf{x}', \quad (24)$$

g being a function which decreases rapidly at infinity. Eq. (24) is a Gabor transform, defining a localized wave-packet at position x with local wavenumber k. The advantage of considering Gabor mode is that it allows simple treatment of dissipation and pressure terms [15]. Note that by construction, $u_i = g(0) \int dk \hat{u}_i(k)$. Here, η_i is a noise, representing the input of energy via the energy cascade. The major approximation of the model is to lump the nonlinear terms describing local interactions into a turbulent viscosity ν^t.

4.3 Reynolds stresses in the quasi-linear approximation

Using the slow variation of $< u >$, we may write the Gabor transform of $Q_{ij} =< u_i > u'_j$ as $< u_i > \hat{u}'_j$. It is then easy to see that the Gabor transform of Q satisfies, in matrix notation:

$$D_t \hat{Q} = -\nu^t \mathbf{k}^2 \hat{Q} + \hat{Q} B^+ + H, \quad (25)$$

where H is a noisy matrix $H_{ij} =< u_i > \eta_j$ and the symbol + means transposed. Decomposing finally B into its symmetric part S and anti-symmetric part A, one obtains finally:

$$D_t \hat{P} = -\nu^t \mathbf{k}^2 \hat{P} + \hat{Q} S + S \hat{Q}^+ + A \hat{Q}^+ - \hat{Q} A + H + H^+,$$
$$D_t \hat{M} = -\nu^t \mathbf{k}^2 \hat{M} + \hat{Q} S - S \hat{Q}^+ + A \hat{Q}^+ + \hat{Q} A + H - H^+, \quad (26)$$

where $P = Q + Q^+$ and $M = Q - Q^+$. One can get physical insights of this system by considering the special case when Q commutes with S and A. In that case, one gets:

$$D_t \hat{P} = -\nu^t \mathbf{k}^2 \hat{P} + SP - AP + H + H^+,$$
$$D_t \hat{M} = -\nu^t \mathbf{k}^2 \hat{M} + SM + AM + H - H^+. \quad (27)$$

It is then easy to see that P and M will behave like a damped oscillator with noise, with damping given by eigenvalues of $S - \nu^t \mathbf{k}^2 I$ and oscillation given by square root of eigenvalues of A^2.

4.4 Application to torque in von Karman

Since $\Gamma_f = \int P_{\phi z}$, we can now use the result on the Reynolds stresses to understand the physical origin, if any, of the various terms appearing in our model (2) and (5). We see that the friction term arises from a combination of turbulent viscosity and symmetrical part of B, i.e. the mean flow stretching. The noise term arises from the energy cascade from large to small scale, while the possible oscillating behavior arises from the anti-symmetrical part of B, i.e. is linked with the mean flow vorticity. For example, if one approximate the von Karman flow by a pure rotating shear flow $< u >= \sigma r z e_\phi$. Its symmetrical tensor S has only two non-zero component, $S_{\phi z} = S_{z\phi} = 0.5 r\sigma$ while the four non-zero components of A are $A_{r\phi} = -A_{\phi r} = -r\sigma$ and $A_{z\phi} = -A_{\phi z} = -0.5 r\sigma$. In that case, $A^2_{z\phi} = 0$ and one can reasonably expect that the same component of P has no oscillatory behavior. This would favor the model EWN (simple damped noise). In realistic von Karman flow, however, a poloidal velocity component is present, due to Ekman pumping. Imagine then that this poloidal field is able to couple linearly u'_z and u'_ϕ through a term like:

$$D_t \hat{u}'_z = \alpha \hat{u}'_\phi. \tag{28}$$

Since u'_ϕ is coupled to u'_z via the differential rotation:

$$D_t \hat{u}'_\phi = \frac{d < u_\phi >}{dz} \hat{u}'_z, \tag{29}$$

this induces a possible oscillatory behavior for $\hat{u}'_z$ and $\hat{u}'_\phi$, hence for Γ'_f.

5 Discussion

In this paper, we studied the injected power in a turbulent device, namely the von Karman swirling flow, by mean of a stochastic model of the turbulent torque. Within this frame, we obtained a few salient results, which were tested and validated on experimental data. Assuming a Gaussian shape with exponential time-correlation of the turbulent torque (EWN model), we recovered the link between variances of power fluctuations in two different forcing regimes (at constant angular velocity and constant applied torque). Moreover, the model was shown to allow for parameter-free prediction of the shape of the PDF of power fluctuations in the case with forcing at constant torque. Further experimental tests of the model are warranted, regarding for example the statistics of the power injected by the turbulence, or the dependence of the model parameter with global quantities. This is left for future work.

We thank O. Cadot and C. Titon for having motivated the present "two-mode" study by experimental considerations and their numerous remarks. We wish also to thank F. Daviaud for his valuable comments and encouragements.

APPENDIX

A Derivation of the Pdf for the angular velocity

In this section, we show how to derive the probability distribution function (Pdf) for Ω verifying the following Langevin equation:

$$\begin{aligned}\frac{d\Omega}{dt} &= \frac{\Gamma_m - c|\Omega|\Omega}{I} + \frac{\xi}{I} \\ \frac{d\xi}{dt} &= -\frac{1}{\tau}\xi + \frac{\eta(t)}{\tau},\end{aligned} \tag{30}$$

where η is a gaussian δ-correlated noise.

This is a non Markovian process which means that no Fokker-Planck equation for the associated distribution can be derived. To overcome this difficulty we used the unified colored noise approximation [35,36] which permits to rewrite the stochastic system in the following way:

$$\frac{d\Omega}{dt} = \frac{\Gamma_m - c|\Omega|\Omega}{\varepsilon(\Omega)} + \frac{\eta(t)}{\varepsilon(\Omega)} \tag{31}$$

with $\varepsilon(\Omega) = I + 2c\tau|\Omega|$. This last equation is now Markovian and we can instantaneously derive a Fokker-Planck equation:

$$\begin{aligned}\frac{\partial P(\Omega,t)}{\partial t} = &-\frac{\partial}{\partial\Omega}\left(\frac{\Gamma_m - c|\Omega|\Omega}{\varepsilon(\Omega)}P(\Omega,t)\right) \\ &+D\frac{\partial}{\partial\Omega}\frac{1}{\varepsilon(\Omega)}\frac{\partial}{\partial\Omega}\frac{1}{\varepsilon(\Omega)}P(\Omega,t)\end{aligned} \tag{32}$$

The stationary distribution follows immediately by integration (equation (13)).

B Moments of the distribution

We want to compute the moment:

$$< \chi^n >= N\int_{-\infty}^{+\infty} f_n(t)\exp[-\frac{1}{R^2}\Phi(t)]dt$$

with:

$$f_n(t) = t^n(|t| + \frac{S}{4}) \tag{33}$$

$$\Phi(t) = (t^2 - \theta(t))^2 - St + \frac{S}{3}\theta(t)t^3 \tag{34}$$

Using Laplace's method up to the second order (cf [38]), we have in the limit $R \ll 1$:

$$\begin{aligned}< \chi^n >= N\sqrt{\frac{2\pi R^2}{\Phi''(t_0)}}e^{-\frac{\Phi(t_0)}{R^2}}[f_n(t_0) - R^2(-\frac{f_n''(t_0)}{2\Phi''(t_0)} \\ +\frac{f_n'(t_0)\Phi'''(t_0)}{2[\Phi''(t_0)]^2} + \frac{f_n(t_0)\Phi''''(t_0)}{8[\Phi''(t_0)]^2} - \frac{5f_n(t_0)[\Phi''(t_0)]^2}{24[\Phi'''(t_0)]^3})]\end{aligned}$$

where t_0 is the minimum of Φ on $]-\infty+\infty[$. For every S, one can show that $t_0 = 1$ and using the fact that $< \chi^0 >= 1$, the following expression is computed:

$$< \chi^n >= 1 - \frac{R^2}{4(4+S)}n(2-n) + O(R^4) \tag{35}$$

For n=2, one get $< \chi^2 >= 1$, which is equivalent to $< \Omega^2 >= \Gamma_m/c$, a trivial relation because it's only the mean part of equation (8). More interesting, one can compute the standard deviation of χ and look at its limit when S (or the inertia) tends to zero:

$$\frac{< \chi^2 > - < \chi >^2}{< \chi >^2} = \frac{R^2}{2(4+S)} + O(R^4) \longrightarrow \frac{R^2}{8} \tag{36}$$

When writing this last equation, in terms of Ω, we recover the equality (16).

References

1. M. Lesieur. *La Turbulence*. Presses universitaires de Grenoble, 1994.
2. E. Hopf. Statistical hydromechanics and functionnal calculus. *J. Rat. Mech. Anal.*, 1:87–123, 1952.
3. A. S. Monin, A. M. Yaglom. *Statistical Fluid Mechanics*. MIT press, Cambridge, 1977.

4. R. Friedrich, J. Peinke. Description of a turbulent cascade by a Fokker-Planck equation. *Phys. Rev. Lett.*, 78(5):863–866, 1997.
5. R. Friedrich, J. Peinke. Statistical properties of a turbulent cascade. *Physica D*, 102(1-2):147–155, 1997.
6. A. Naert, B. Castaing, B. Chabaud, B. Hebral, J. Peinke. Conditional statistics of velocity fluctuations in turbulence. *Physica D*, 113(1):73–78, 1998.
7. P. Marcq, A. Naert. A Langevin equation for turbulent velocity increments. *Phys. Fluids*, 13(9):2590–2595, 2001.
8. A. M. Obukhov. Description of turbulence in terms of Lagrangian variables. *Adv. Geophys.*, 6:113–116, 1959.
9. B. Castaing, Y. Gagne, E. J. Hopfinger. Velocity probability density functions of high Reynolds number turbulence. *Physica D*, 46:177–200, 1990.
10. J. Delour, J.-F. Muzy, A. Arneodo. Intermittency of 1D velocity spatial profiles in turbulence: a magnitude cumulant analysis. *Eur. Phys. J. B*, 23(2):243–248, 2001.
11. R. Friedrich. Statistics of Lagrangian velocities in turbulent flows. *Phys. Rev. Lett.*, 90(8):084501, 2003.
12. C. Beck. Lagrangian acceleration statistics in turbulent flows. *Europhys. Lett.*, 64(2):151–157, 2002.
13. J.-P. Laval, B. Dubrulle, S. Nazarenko. Nonlocality of interaction of scales in the dynamics of 2D incompressible fluids. *Phys. Rev. Lett.*, 83(20):4061–4064, 1999.
14. J. Carlier, J.-P. Laval, J. M. Foucaut, M. Stanislas. Nonlocality of the interaction of scales in high reynolds number turbulent boundary layer. *C. R. Acad. Sci., Ser. B*, 329:1–6, 2001.
15. J.-P. Laval, B. Dubrulle, S. Nazarenko. Non-locality and intermittency in 3D turbulence. *Phys. Fluids*, 13:1995–2012, 2001.
16. B. Dubrulle, S. Nazarenko. Interaction of turbulence and large-scale vortices in incompressible 2D fluids. *Physica D*, 110:123–138, 1997.
17. S. Nazarenko, N. K.-R. Kevlahan, B. Dubrulle. A WKB theory for rapid distortion of inhomogeneous turbulence. *J. Fluid Mech.*, 390:325, 1999.
18. J.-P. Laval, B. Dubrulle, S. V. Nazarenko. Dynamical modeling of sub-grid scales in 2D turbulence. *Physica D*, 142:231–253, 2000.
19. B. Dubrulle, J.-P. Laval, S. Nazarenko, N.K.-R. Kevlahan. A dynamic subfilter-scale model for plane parallel flows. *Phys. Fluids*, 13:2045–2064, 2001.
20. A. A. Townsend. *The structure of turbulent shear flows*. CUP, 1976.
21. J. F. Keffer, J. G. Kawall, J. C. R. Hunt, M. R. Maxey. Uniform distrortion of thermal velocity mixing layers. *J. Fluid Mech.*, 86:465–490, 1978.
22. M. R. Maxey. Distortion of turbulence in flows with parallel streamlines. *J. Fluid Mech.*, 124:261–282, 1981.
23. N. K.-R. Kevlahan. Rapid distortion of turbulent structures. *Appl. Sci. Res.*, 51:411–415, 1993.
24. N. K.-R. Kevlahan, J. C. R. Hunt. Nonlinear interactions in turbulence with strong irrotational straining. *J. Fluid Mech.*, 337:333–364, 1997.
25. J.-P. Laval, B. Dubrulle, J.C. Mc Williams. Langevin models of turbulence: Renormalization group, distant interaction algorithms or rapid distortion theory ? *Phys. Fluids*, 15(5):1327–1339, 2003.
26. R. Labbé, J.-F. Pinton, S. Fauve. Power fluctuations in turbulent swirling flows. *J. Phys. II (Paris)*, 6:1099–1110, 1996.

27. O. Cadot, Y. Couder, A. Daerr, S. Douady, A. Tsinober. Energy injection in closed turbulent flows: stirring through boundary layers versus inertial stirring. *Phys. Rev. E*, 56:427–433, 1997.

28. S. Aumaitre, S. Fauve, J.-F. Pinton. Large scale correlations for energy injection mechanisms in swirling turbulent flows. *Eur. Phys. J. B*, 16:563–567, 2000.

29. J.-H. C. Titon, O. Cadot. The statistics of power injected in a closed turbulent flow: constant torque forcing vs constant velocity forcing. *Phys. fluids*, 15(3):625–640, 2003.

30. S. Aumaitre, S. Fauve, S. McNamara, P. Poggi. Power injected in dissipative systems and the fluctuation theorem. *Eur. Phys. J. B*, 19, 2001.

31. R .S. Ellis. *Entropy, Large deviations and statistical mechanics*. Springer Verlag, New York, 1985.

32. Y. Oono. Non-equilibrium statistical mechanics: large deviation theory. *Progr. Theor. Phys. Suppl.*, 99, 1989.

33. L. Marié, F. Daviaud. Experimental measurement of the scale-by-scale momentum transport budget in a turbulent shear flow. *Phys. Fluids*, 16(2):457–461, 2004.

34. P. E. Kloeden, E. Platen. *Numerical solution of stochastic differential equations*. Springer-Verlag, 1992.

35. P. Jung, P. Hänggi. Dynamical systems: a unified colored-noise approximation. *Phys. Rev. A*, 35(10):4464–4466, 1987.

36. S. Z. Ke, D. J. Wu, L. Cao. Phase transitions in a bistable system driven by two colored noises. *Eur. Phys. J. B*, 12:119–122, 1999.

37. J-F. Pinton, P.C. Holdsworth, R. Labbé. Power fluctuations in a closed turbulent shear flow. *Phys. Rev. E*, 60:R2452–R2455, 1999.

38. C. M. Bender, S. A. Orszag. *Advanced mathematical methods for scientists and engineers*. Mc Graw Hill, 1975.